Sustainable Energy, Grids and Networks 10 (2017) 35–45

Contents lists available at ScienceDirect

Sustainable Energy, Grids and Networks

journal homepage: www.elsevier.com/locate/segan

Feeder dynamic rating application for active distribution network using synchrophasors

Narender Singh *, Hossein Hooshyar, Luigi Vanfretti

KTH Royal Institute of Technology, Sweden

ARTICLE INFO

Article history:
Received 13 July 2016
Received in revised form
17 February 2017
Accepted 17 February 2017
Available online 22 February 2017

Keywords:
Active distribution networks
Dynamic line rating
IEEE 738
Kalman filter
Real-time hardware-in-the-loop simulation
Synchrophasors

ABSTRACT

Dynamic line rating (DLR) has found acceptance and increasing application in transmission network as a means to utilize the maximum capability of existing transmission lines. With the increasing number of generation sources at lower voltage levels, DLR may be of value for aerial MV feeders for similar purposes and to gain insight on the operation of generation sources at lower voltage levels. Static line ratings are based on a conservative estimate, which means that on most occasions, the actual capacity of lines is higher than the static line ratings. In order to exploit DLR in lower voltage levels, this paper introduces a method developed to exploit different data sources, including real time weather conditions, conductor sag and the actual line loading of the conductor to provide dynamic line ratings for active distribution networks. The method has been implemented in a software application in the LabVIEW environment and provides a user friendly front panel where real-time ampacity can be seen compared to the actual line loading. The developed application has been assessed through a hardware-in-the-loop (HIL) simulation setup. In addition, dynamic line rating results from the application have been appraised against those of proprietary solutions available in the market.

1. Introduction

During the past decade, there has been a consistent increment in electricity demand that is not likely to stabilize or reverse in near future. According to some statistics reported in [1], the period of 2003–2013 has witnessed an increment of 5.1% in household electricity consumption in European Union member states. This growth is as high as 25% in some member states. Needless to say, this growth in electricity consumption is even higher in developing countries. India is one such example where an estimated increase in electricity consumption from 411,887 GWh during 2005–2006 to 882,592 GWh during 2013–2014 was registered [2]. Moreover, extension of existing transmission and distribution networks require consent from the authorities and a significant investment. This can take several years to be implemented. Adding to these circumstances the increase of generation installations at lower voltage levels that pose challenges for grid operation [3] results in increased pressure on electric utilities to make optimum use of existing facilities [4].

1.1. Motivation

Dynamic Line Rating (DLR) systems provide information that can enhance the use of power transmission and distribution assets. DLR is a method that can enhance the use of power transmission and distribution lines not only by scrutinizing the electrical current passing through them but also by taking into account the effects of environmental variables such as wind speed, wind direction, solar radiation and ambient temperature [5]. According to US Department of Energy, all transmission owners and operators calculate static ratings for their lines based on worst-case scenarios (low wind speed, high ambient temperature and high solar radiation) [6]. On the other hand, dynamic thermal rating of a conductor (i.e. the conductor current that produces maximum allowable conductor temperature at a specific location and time along the power line [7]) can be computed by DLR systems in order to utilize the conductor full capacity. Making better use of the "ampacity" using these systems has shown to return annual benefit of 35,000 USD/GWh as compared to conductor upgrading and the construction of new line which give an economic benefit of 17,000 USD/GWh and 11,000 USD/GWh, respectively [8].

DLR systems can also be utilized for several different applications such as security constrained unit commitment, optimal power flow, line rating forecasting, and need-based maintenance of lines instead of the traditional time-based maintenance [9–11].

* Corresponding author.
E-mail addresses: nsingh@kth.se (N. Singh), hosseinh@kth.se (H. Hooshyar), luigiv@kth.se (L. Vanfretti).

http://dx.doi.org/10.1016/j.segan.2017.02.004
2352-4677/

In addition, monitoring conductor rating versus its loading in active distribution networks is a critical task when dealing with bi-directional power flows, due to the presence of Distributed Generation (DG), which can cause the feeders to be overloaded [12].

1.2. Literature review

There have been significant developments in the field of dynamic line rating with a main focus on transmission lines. These developments have become possible as a result of relatively inexpensive, reliable and accurate instruments available to measure weather, line sag-tension and conductor temperature [13]. The existing DLR systems can be categorized into four groups as detailed below:

1.2.1. Weather dependent systems

These systems are based upon weather variables. To accurately obtain line ratings from a weather dependent system, it is important to ensure real-time access to a weather station in the vicinity to the line of interest. This weather station should be equipped with an anemometer, wind direction sensor, solar radiation sensor and temperature sensor as explained in [14].

1.2.2. Temperature dependent systems

The temperature dependent systems work using direct measurement of the conductor's temperature. For this purpose, a device needs to be installed to determine the conductor temperature in real-time. A study conducted to evaluate one of such devices has been reported in [15]. The device studied accurately measured the line current, conductor temperature and ambient temperature. The installed system consists of sensors mounted directly on the conductor of interest or at a station bus.

1.2.3. Tension monitoring systems

Tension monitoring system is another technique to determine the ampacity of a line by making use of measurements of conductor's tension along the line. These systems rely on the principle that conductor tension is a function of conductor temperature. This method is especially useful in different loading conditions as the effect of ice and wind loading can be considered. One disadvantage of this monitoring system is that during the installation and maintenance of the system, the line has to be taken out of service [16].

1.2.4. Sag dependent systems

These systems make use of real-time sag measurement of the conductor. As discussed in [17], laser or radar scanning are some of the methods available for sag measurement. Studies in [18,19] also introduce some other methods for sag monitoring. These systems are usually equipped with an alarming system that helps to maintain the sag clearance level, which should at no time exceed the permissible limit for safe operation. An offline monitoring system that does not require the installation of any device on the line is presented in [16]. Here, the sag is measured using a laser beam and that detects the lowest point of the conductor from ground. By knowing the value of conductor sag and with knowledge of ambient weather conditions it is possible to calculate the real-time ampacity of the line of interest.

Examples of the above-mentioned systems can be found widely in the literature. The study reported in [20,21] uses PMU measurements to estimate the line's temperature and sag. The PMU data (positive sequence currents and voltages) at both ends of the line are used to derive its corresponding positive sequence impedance. This impedance is then used to estimate the value of conductor's temperature and thereby its real-time ampacity. Although this is an interesting method that makes use of PMU data for DLR estimation, it cannot be utilized for distribution systems. This is because distribution systems cannot be represented by positive sequence networks as they are highly unbalanced. This unbalance is due to the fact that line transposition is uneconomic and sometimes physically impossible in distribution systems. In addition, individual phase load levels are always changing, and consequently perfect loading is never achieved [22].

Ref. [23] introduces a device that is mounted directly on the line to measure the conductor's surface temperature from where the real-time ampacity is computed. This device provides reasonable accuracy, however it may be uneconomic for distribution systems due to phase unbalances that would lead to unequal temperatures, thus requiring individual devices for each phase.

The DLR system presented in [15] measures the feeder conductor's current and temperature. These measurements are then transmitted through a telephony channel to a receiver that computes the real-time ampacity. Although this method is efficient, it is not suitable for a distribution networks because the range of conductor current that can be measured by this device is from 250 A to 2000 A, whereas in distribution networks the line currents can be much lower.

In [24], a DLR system using a tension monitoring system is presented. This method requires tension monitors installed between dead-end insulators and line structures. One advantage of using this method is that the measured conductor tension can be used to compute sag using ruling span theory. With all the advantages of this system, what makes it uneconomic for distribution network is that because of phase load unbalances, it is possible that different phases have a different tension. Therefore, to monitor all phases, multiple devices need to be installed.

In [25], a sag dependent system is introduced and has been successfully tested on a distribution line. The method uses a GPS positioning sensor to monitor the distribution feeder sag. The system has a relatively low cost making it suitable for distribution systems.

Table 1 shows a brief comparison between the various DLR monitoring techniques discussed above. By comparing costs, it is clear that all the systems mentioned above (except for the last one) are quite expensive and therefore will be costly to apply in distribution networks.

1.3. Paper contributions

Over the years many Dynamic Line Rating systems for transmission systems have been developed. However, their potential application in distribution networks has (comparatively) been neglected. As explained in the previous section, distribution systems have the distinct characteristic of unbalances. As a result, the developed DLR systems are either inappropriate or too costly for their use in distribution networks as compared with transmission networks.

This paper proposes DLR algorithm for active distribution systems whose overall cost can be lower by exploiting different data sources. The proposed algorithm relies on the GPS positioning sensor introduced in [25], for sag estimation and, makes use of both IEEE 738 standard [29] and the State Change Equation [30] to reliably estimate the conductor temperature. Hence, the temperature is determined by two methods, whose outputs are processed by a Kalman filter. The result is used together with weather data and conductor loading to determine the conductor's real-time ampacity. As the algorithm is intended for active distribution systems, PMU measurements are used to provide time-tagged values of the conductor loading to capture the dynamics of the system. The proposed algorithm is implemented

Table 1
Different DLR techniques and their cost.

Method	Brief introduction	Pros	Cons	Cost
Proprietary method 1 [23]	A temperature dependent system first developed in 1988 has over 1000 installations.	– Powered directly from the measured conductor – Mature device, has been in use for many years	– Expensive setup	– Configuration dependent, one location system can cost US$40,000–$80,000
Proprietary method 2 [26]	Tension dependent system installed by over 100 utilities.	Reduced price with wide deployment	– Span lengths should not differ greatly with ruling span section – Insulator string should be relatively long. – Structure should be rigid	€2500–3000 per circuit km
Proprietary method 3 [27]	Sag dependent system with over 80 units installed in North America.	– High accuracy (±15 mm)	– Extreme weather conditions like fog, heavy snow may compromise the measurement	Undisclosed
Proprietary method 4 [28]	Sag dependent system with a smart sensor module directly deployed on the overhead line. Analyzes conductor vibrations and detects fundamental frequencies of the span.	– No calibration required – Does not require external power source	– The minimum level of current is 80 A which makes it unsuitable for distribution network	€40,000 + €10,000 per line for real-time measurements + data hosting services (extra)
GPS based system	Sag measuring system	– Economic option. – Tested for distribution networks	– Measurements need to be filtered	GPS device cost (BT-359): $ 50

in the LabVIEW platform and has been assessed through HIL simulation experiments.

The paper begins with a thorough explanation on the proposed dynamic line rating algorithm in Section 2. In Section 3, the developed LabVIEW application and the HIL simulation setup, through which the application is assessed, are presented. Section 4 includes a performance analysis of the developed application. Conclusions and future work are included in Section 5.

2. Dynamic line rating in active distribution networks

This section explains the main blocks that comprise the proposed DLR algorithm for active distribution networks.

2.1. IEEE 738 standard

IEEE 738 is a standard for calculating the current–temperature relationship of conductors from the knowledge of ambient conditions [29]. The standard mainly stands on (1), that is a non-steady state heat balance equation.

$$q_c + q_r + mC_p \frac{dT_c}{dt} = q_s + I^2 R\,(T_c) \tag{1}$$

where q_c is the rate of heat loss due to convection, q_r is the radiated heat loss, mC_p is heat capacity of the conductor, T_c is the conductor temperature, q_s is the solar heat gain, I is current through the conductor and $R(T_c)$ is the resistance of conductor at temperature T_c. More details on the standard can be found in [29].

There are two ways in which this standard can be used. Assuming that the ambient condition is known, the standard can be used to calculate the current that corresponds to a known conductor temperature. In addition, when the current through the conductor is known, it can be used to calculate the conductor's temperature. In other words, (1) is a relationship between the actual current through the conductor and its temperature. This equation can also be used to calculate the ampacity of the conductor that can be defined as the current that lead to reach the maximum allowed temperature in the conductor in specified time span. The ampacity calculation in such manner requires the knowledge of the initial temperature of conductor in the steady state.

2.2. State change equation

State change equation relates the conductor temperature to the span sag. The state change equation in its general form is a cubic polynomial function that is solved using numerical methods. However, it is also possible to write it for direct calculation as follows.

$$\sigma^3 - \sigma^2 \left(\sigma_0 - \alpha E\,(t - t_0) - \frac{a^2 g_0^2 E}{24\sigma_0^2} \right) = \frac{a^2 g^2 E}{24} \tag{2}$$

where σ and σ_0 are the stress in final and initial state respectively, α is the coefficient of thermal expansion, E is the modulus of elasticity, t and t_0 are the temperature in final and initial state respectively, a is the span length of the conductor and g and g_0 are the specific load in final and initial state respectively. More details on the equation can be found in [30].

2.3. Kalman filter

The Kalman filter is an optimal recursive estimator used to determine unknown variables with better precision than using only direct measurements. Considering the data of interest (i.e. the conductor temperature in this case — to be explained in the next section) as states of a linear discrete time process, the measurements (i.e. the temperature computed from the conductor sag measurements in this case — to be explained in the next section) can be related to the data of interest using linear stochastic process and measurement equations as stated in (3).

$$\begin{aligned} \boldsymbol{x}_k &= \boldsymbol{A}\boldsymbol{x}_{k-1} + \boldsymbol{B}\boldsymbol{u}_k + \boldsymbol{w}_{k-1} \\ \boldsymbol{z}_k &= \boldsymbol{H}\boldsymbol{x}_k + \boldsymbol{v}_k \end{aligned} \tag{3}$$

where $\boldsymbol{x}$ is the state vector, $\boldsymbol{z}$ is the measurement vector, A is the $n \times n$ matrix that relates the state at previous time step $k-1$ to the state at current step k, which is assumed to be constant in each iteration, $\boldsymbol{B}$ is the control input which relates input $\boldsymbol{u}$ to the state $\boldsymbol{x}$ and $\boldsymbol{H}$ is the $m \times n$ matrix which relates state $\boldsymbol{x}_k$ to the measurements $\boldsymbol{z}_k$. The process noise $\boldsymbol{\omega}_k$ and measurement noise $\boldsymbol{v}_k$ are assumed to be two mutually independent random variables with normal probably distributions

$$\begin{aligned} p(\boldsymbol{w}) &\sim N(0, \boldsymbol{Q}) \\ p(\boldsymbol{v}) &\sim N(0, \boldsymbol{R}) \end{aligned} \tag{4}$$

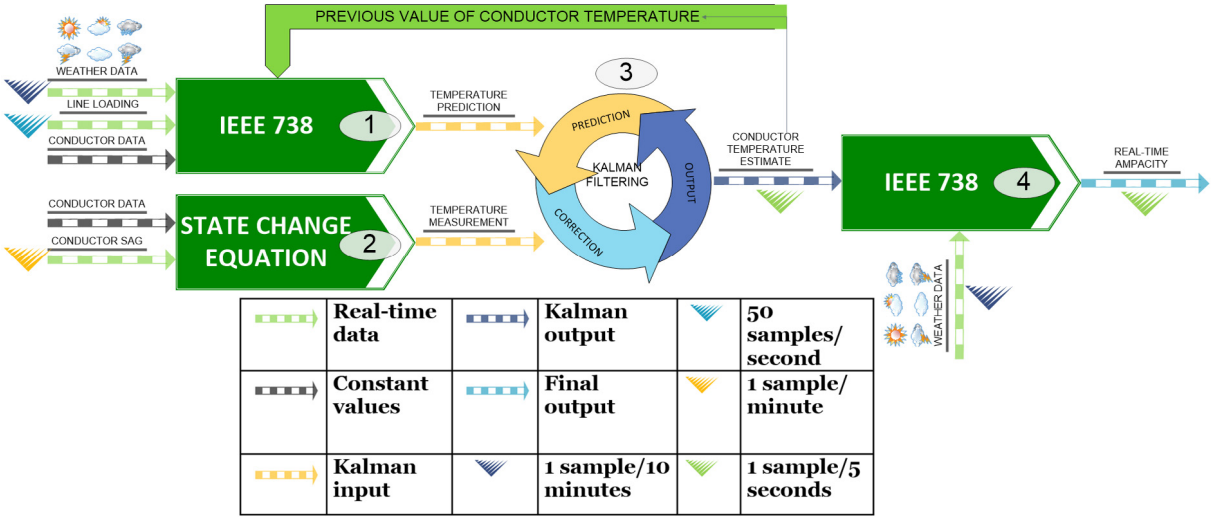

Fig. 1. Block diagram of the proposed DLR algorithm.

where $\boldsymbol{Q}$ is the process noise covariance matrix and $\boldsymbol{R}$ is the measurement noise covariance matrix.

The Kalman filter includes main stages, namely, 'prediction' and 'correction'. The steps involved in these two stages are listed in Table 2.

The 'prediction' of the state (the unknown variable) is basically the forward projection in time of the previous state $\hat{\boldsymbol{x}}_{k-1}$ and the error covariance estimate $\boldsymbol{P}_{k-1}$ to obtain the a priori state estimates $\hat{x}_{\boldsymbol{k}}^{-}$ and the a priori error covariance estimate $\boldsymbol{P}_{k}^{-}$ for the next step k.

In the 'correction' stage, new measurement ($\boldsymbol{z}_k$) is incorporated into the priori estimate ($\hat{x}_{\boldsymbol{k}}^{-}$) to obtained a posteriori estimate ($\hat{x}_{\boldsymbol{k}}$). The posteriori estimate has always higher certainty compared to both the predicted priori state ($\hat{\boldsymbol{x}}_{k-1}$) and the measured value of the state ($\boldsymbol{z}_k$).

A detailed explanation of Kalman filter can be found in [31].

2.4. DLR algorithm for active distribution systems

Fig. 1 illustrates the block diagram of the proposed DLR algorithm. As shown in the figure, the ampacity calculation relies upon real-time inputs of line sag from the GPS positioning sensor, ambient weather conditions from a nearby weather station and line loading from PMUs. In addition, the algorithm requires conductor data, including conductor weight, diameter, heat capacity, resistance per meter, etc., that are constant and are not subjected to any significant change over time. Note that the GPS positioning sensor needs to be hanged at mid span of the feeder of interest to measure the conductor sag. More details can be found in [25].

As shown in Fig. 1, the algorithm is initiated by feeding the real-time conductor sag measurement to the state change equation block that allows to solve for an estimate (termed herein as 'measurement') which enables an indirect measurement of the conductor's temperature (number 2 in Fig. 1). However, as the sag measurement may contain errors due to GPS-inaccuracies or sensor's inaccurate positioning, the conductor temperature obtained from the state change equation should not be directly used to compute the real-time ampacity.

Another mean to obtain an estimate of the conductor's temperature is to use the IEEE 738 standard. In this work, the IEEE 738 standard is used to predict the conductor's temperature (number 1 in Fig. 1) in each time step using the time derivative of (1) and the last estimated value of the conductor temperature, as shown in Fig. 1. This actually forms the prediction step of the proposed Kalman filter as the 'predicted' value is basically the forward projection in time of the previously estimated conductor temperature.

The 'measurement' estimated using the state change equation and the 'predicted' value from the IEEE 738 standard are merged using a Kalman filter to produce a more accurate estimate of the conductor temperature (number 3 in Fig. 1). The Kalman filter not only improves the certainty of the estimates but it is exploited here as a tool to merge data that is updated at different rate. As shown in Fig. 1, while the line loading is updated 50 samples/second by PMUs, the conductor sag measurement and ambient conditions are available at 1 sample/minute and 1 sample/10 min, respectively. While merging two inputs, the Kalman filter uses sample-and-hold technique for the input with the slower updating rate. Fig. 2 compares a conductor temperature profile occurring in a distribution system before and after Kalman filtering. The raw and filtered conductor temperatures are also compared to the conductor's temperature "true values" (i.e. not contaminated with noise). As the figure shows, the Kalman-filtered profile shows a smoother profile with less noise and closer to that of the "true values". Note that the accuracy of the Kalman-filtered temperature is influenced by the measurement and process noise covariance matrices, i.e. $\boldsymbol{R}$ and $\boldsymbol{Q}$. These two matrices are respectively dependent on the accuracy of the measurement (that is in our case the indirectly measured temperature coming from the GPS device through the state change equation) and the predicted temperature (coming from the previously estimated temperature through the IEEE 738 standard). In this study, we have assumed that both temperatures have the same amount of accuracy, i.e. $\boldsymbol{R} = \boldsymbol{Q}$; however, they should be readjusted when it is needed. For example, if the GPS device gives noisy values, $\boldsymbol{R}$ should be increased.

Having an accurate estimate of the conductor temperature from the Kalman filter, the IEEE 738 standard, i.e. Eq. (1), is brought to use again; this time to calculate ampacity of the conductor (number 4 in Fig. 1). Apart from the conductor temperature, provided by the Kalman filter, other required inputs are the conductor constants, real-time weather conditions and actual line loading from the PMUs.

Note that because the active distribution networks may be highly unbalanced, it is important to apply this algorithm for each phase individually. The next section presents the developed DLR application in the LabVIEW environment and its assessment through a HIL simulation setup.

Table 2
Kalman filter algorithm steps.

Step		Equation	Significance
1	Prediction	$\hat{x}_k^- = A\hat{x}_{k-1}^- + Bu_k$	Project the state ahead.
2		$P_k^- = AP_{k-1}A^T + Q$	Project the error covariance ahead.
3	Correction	$K_k = P_k^- H^T \left(HP_k^- H^T + R\right)^{-1}$	Compute the Kalman gain.
4		$\hat{x}_k = \hat{x}_k^- + K_k(z_k - H\hat{x}_k^-)$	Update estimate with measurement z_k.
5		$P_k = (I - K_k H)\, P_k^-$	Update the error covariance.

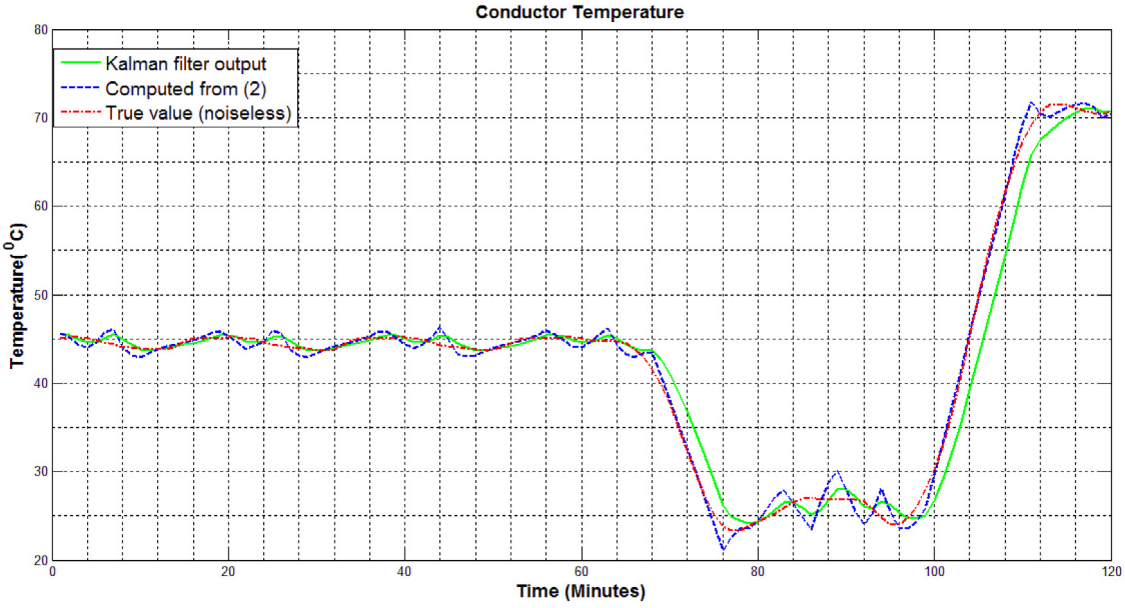

Fig. 2. Kalman filtering results for the conductor temperature.

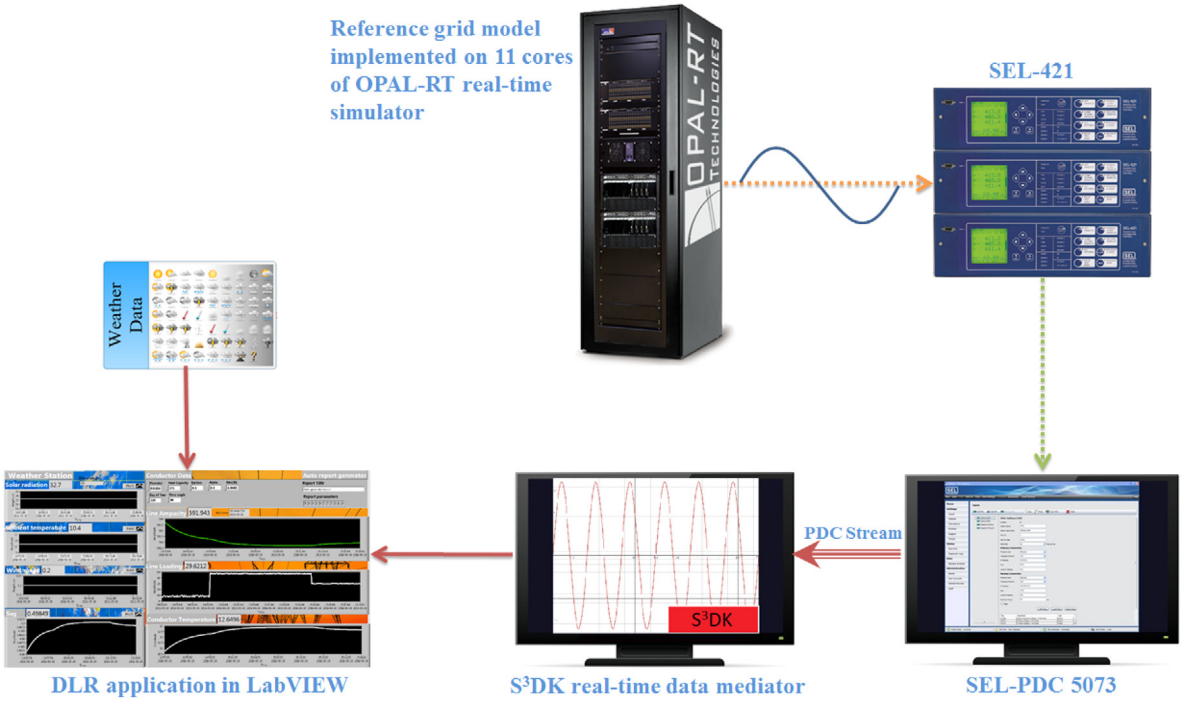

Fig. 3. HIL simulation setup.

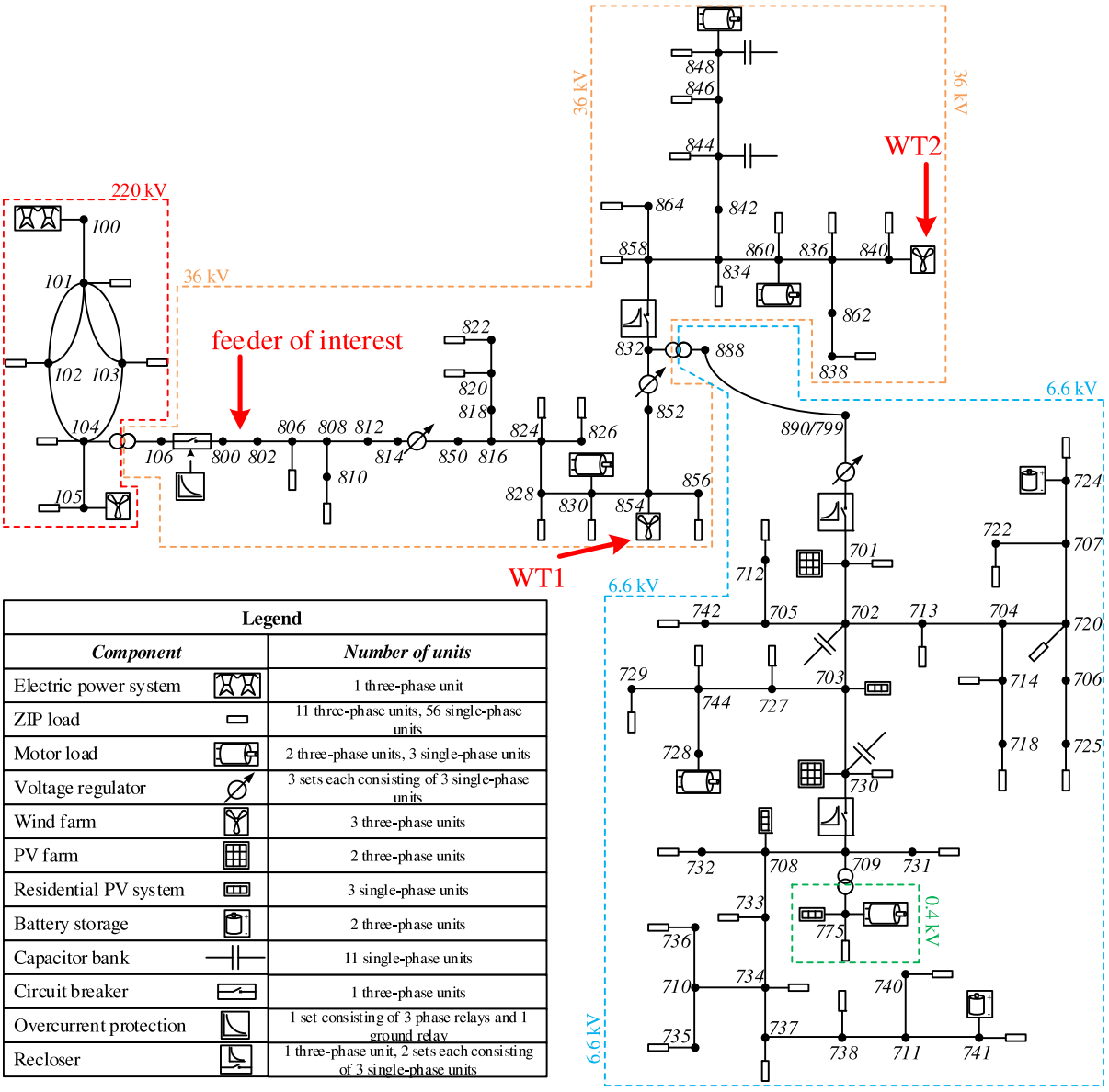

Legend	
Component	*Number of units*
Electric power system	1 three-phase unit
ZIP load	11 three-phase units, 56 single-phase units
Motor load	2 three-phase units, 3 single-phase units
Voltage regulator	3 sets each consisting of 3 single-phase units
Wind farm	3 three-phase units
PV farm	2 three-phase units
Residential PV system	3 single-phase units
Battery storage	2 three-phase units
Capacitor bank	11 single-phase units
Circuit breaker	1 three-phase units
Overcurrent protection	1 set consisting of 3 phase relays and 1 ground relay
Recloser	1 three-phase unit, 2 sets each consisting of 3 single-phase units

Fig. 4. The EU IDE4L project model from active distribution grid [33].

3. Real-time HIL experiment

3.1. HIL simulation setup

The proposed algorithm has been implemented using both programming and graphical tools available in the LabVIEW environment. Fig. 3 shows the HIL setup used to assess the performance of the developed application. As shown in the figure, a reference active distribution grid, designed and implemented in [32], has been used to conduct real-time HIL experiments using the OPAL-RT real-time simulator. The grid, as shown in Fig. 4, is a 79 bus multi-phase network including numerous components of 10 different types, each with electrical and mechanical parts, various controllers and protection systems, to emulate the behavior of an active distribution grid. More details on the grid model can be found in [33]. As highlighted in Fig. 4, the feeder of interest in this study is the one between nodes 800 and 802. Hence, the measured currents of this feeder are fed to the low-level inputs of the PMUs through the analogue output ports of the OPAL-RT simulator. The PMUs used in this setup are SEL-421 from Schweitzer Engineering Laboratories.

The PMU data are then sent to a Phasor Data Concentrator (PDC) that streams the data over TCP/IP to a workstation computer holding Statnett's Synchrophasor Development Kit (S^3DK) [34], which provides a real-time data mediator that parses the PDC data stream and makes it available to the user in the LabVIEW environment. Utilizing functions provided by the S^3DK, the DLR algorithm was implemented in LabVIEW.

As real-time weather data (i.e. wind speed, wind direction, solar radiation and ambient temperature) is critical for the algorithm to work, a LabVIEW interface was used to directly connect to a weather station and receive regularly updated measurements.

Note that because the developed application is not monitoring an actual feeder, the sag data was obtained through a look-up table containing the assumed sag–temperature chart of the feeder conductor.

3.2. Test scenario and results

Fig. 5 shows a screenshot of the front panel of the developed DLR application. The left portion of the figure represents the weather station and the sag monitoring section of the application. Here, the

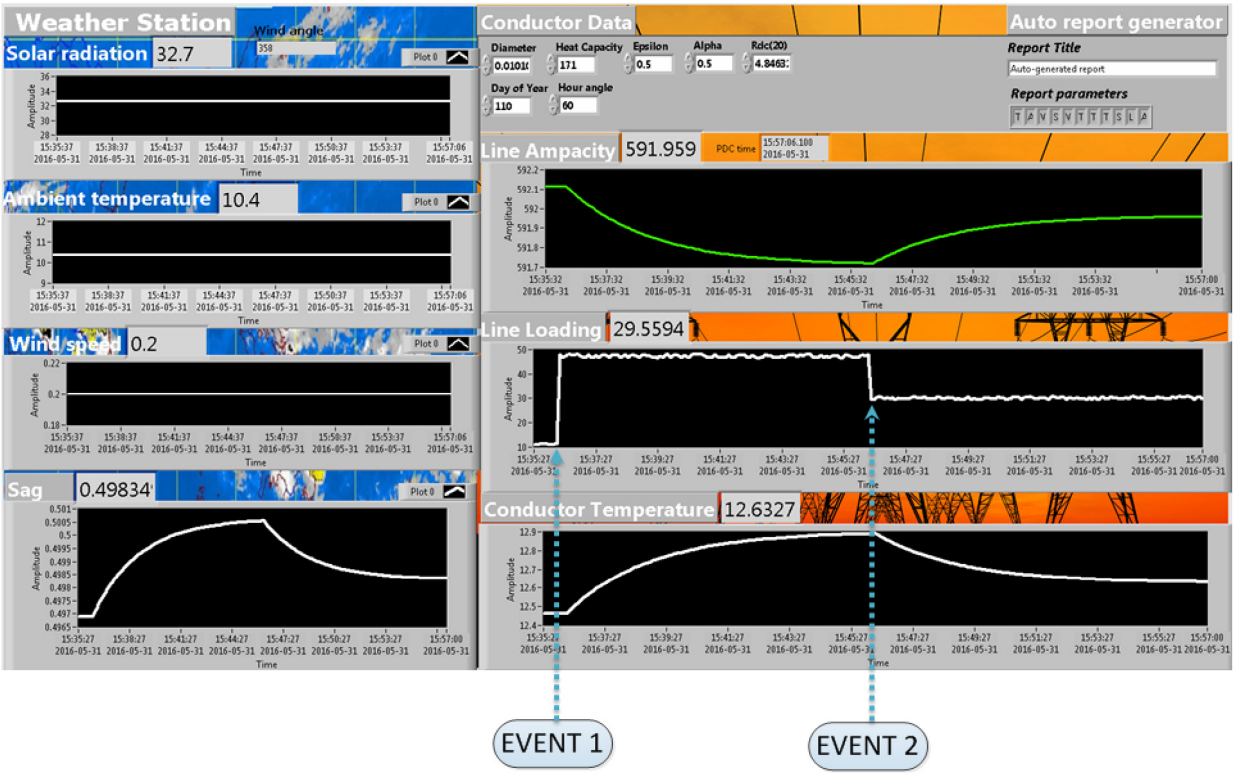

Fig. 5. Screenshot of the developed DLR application tested using RT-HIL experiments.

measurements received in real-time are displayed in a graph. The right portion of the figure displays the line loading, provided by the PMUs, and the real-time conductor temperature and ampacity, computed by the DLR algorithm.

As indicated in the figure, there are two main events that influence the line loading and cause a change in the line ampacity. The first event is when two wind generation units, connected to the MV section and highlighted as WT1 and WT2 in Fig. 4, shut down simultaneously. This causes a sudden loss of around 2 MW generation which leads to an increase in the line current flowing through the feeder of interest. The line current, in turn, causes more heat loss and larger conductor sag, as shown in the figure. With an increase in the conductor sag, the conductor temperature computed by the algorithm increases resulting in a lower ampacity of the conductor. Note that the change in conductor temperature is not sudden, rather it is a gradual change depending on the conductor properties, in particular its heat capacity.

In the second event, one of the wind turbines (i.e. WT2) connects back to the grid, thus reducing the line current and increasing the line ampacity. Note that in this test scenario the ambient conditions are constant and weather conditions are not suffering any noticeable variation.

The application saves all inputs and outputs with their time-tags in Excel table sheets for further offline analysis.

4. Qualitative analysis of the developed application

4.1. Qualitative input–output correlation

Dynamic line rating of a conductor is influenced by various ambient conditions, conductor sag and line loading. The ampacity of the line is therefore correlated with these factors. In Section 3.2, it was shown that the line ampacity is inversely correlated with the line loading and conductor sag. In this section, the variation of the line ampacity, as the output of the developed application, is compared against the variations in weather data. For this purpose, the application was executed for a relatively longer time period (compared to the test scenario in Section 3.2) to capture the effect of weather and the Excel sheets generated by the application have been used for a qualitative correlation analysis. The tests have been performed on an actual line located close to Liden, Sweden [35] using the weather data provided by a nearby weather station.

Fig. 6 shows the line ampacity versus solar radiation. It is clear from the figure that the ampacity has a negative (inversely proportional) correlation with solar radiation: with increasing solar radiation the line ampacity decreases. Fig. 7 shows the ambient temperature versus line ampacity. It can be observed that the line ampacity decreases with increasing ambient temperature. Fig. 8 compares the line ampacity against wind speed, it is not clear what the impact of this variable is on ampacity visible. This is due to the fact that the analyzed data comes from a cold region with temperature <20 °C, under such conditions the heat dissipating impact of wind is almost negligible. This phenomenon is further explained in the next section.

4.2. Qualitative sensitivity analyses

In this section, a qualitative sensitivity analysis is carried out to analyze the impact of different inputs on the main output (ampacity) computed by the developed application. The analysis is performed by isolating the impact of each type of input measurement source. This was carried out by keeping the input measurement source under analysis at a constant value equivalent to its average value during the period of analysis, and then comparing the resulting line ampacity with the ampacity computed originally.

Figs. 9–11 compare the ampacity computed originally against the ampacity computed with:

- Constant solar radiation
- Constant ambient temperature
- Constant wind speed.

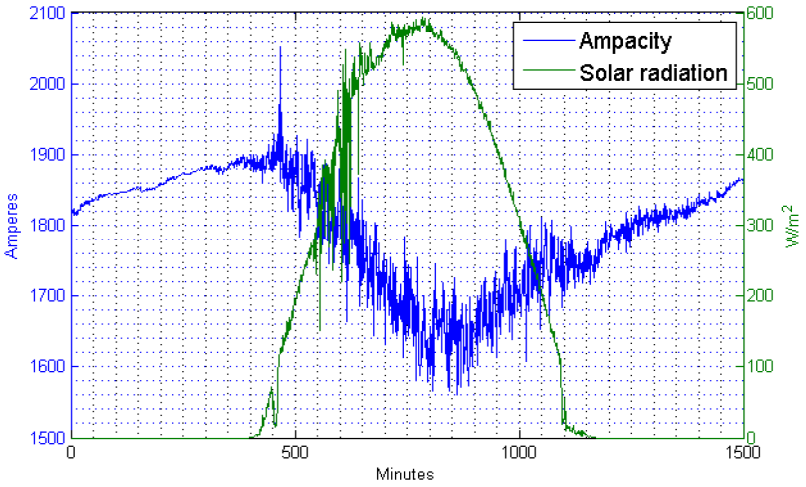

Fig. 6. Ampacity vs. solar radiation.

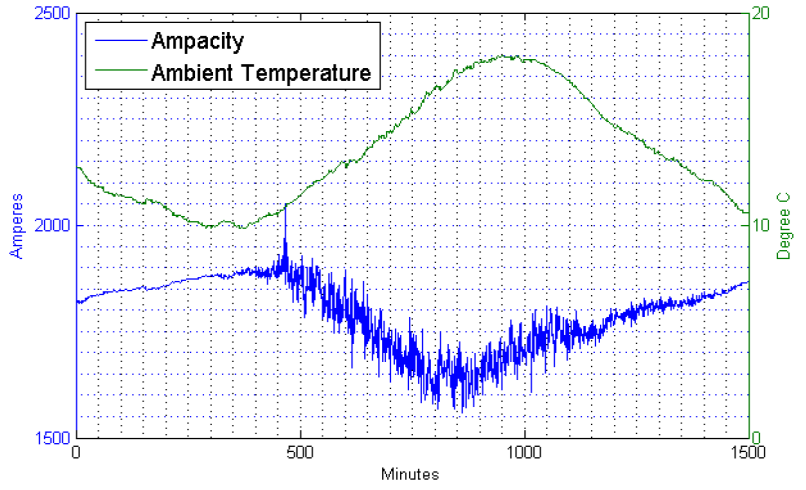

Fig. 7. Ampacity vs. ambient temperature.

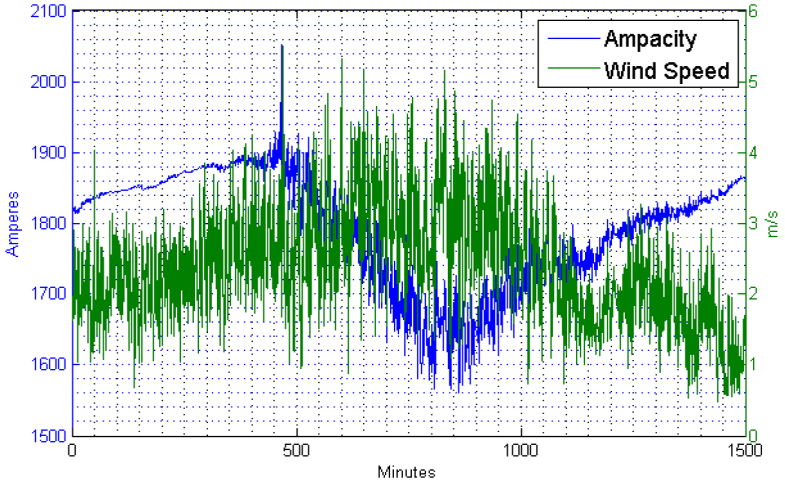

Fig. 8. Ampacity vs. wind speed.

As the figures indicate, the ampacity computed by the developed application is most sensitive to the ambient temperature. In addition, wind speed does not impact the ampacity noticeably. As discussed in the previous section, for cold regions the wind does not play an important role on cooling down the conductor, and therefore it does not significantly impact the computed ampacity. An important implication of such conclusion is that the ampacity calculation can be simplified under similar ambient conditions by ignoring wind variations.

Figs. 12 and 13 depict the impact of line loading and sag on the computed ampacity, respectively. As the figures show, the ampacity computed under follows the original ampacity relatively

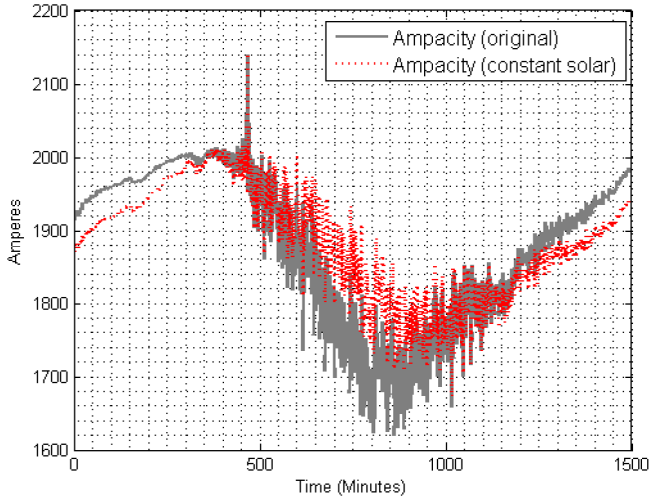

Fig. 9. Impact of solar radiation in the ampacity calculation ampacity.

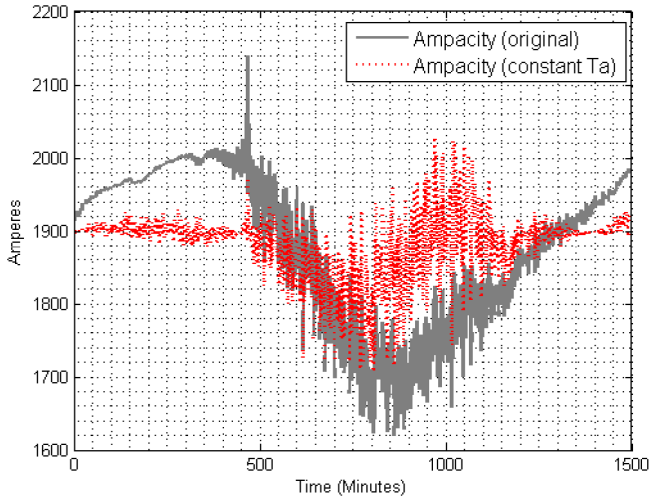

Fig. 10. Impact of ambient temperature in the ampacity calculation.

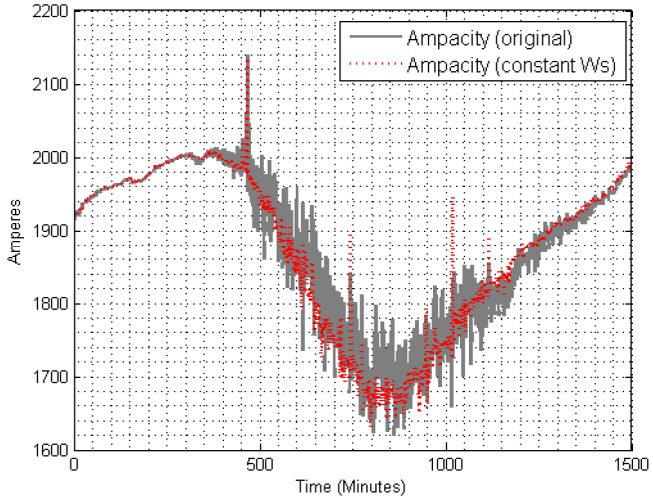

Fig. 11. Impact of wind speed in the ampacity calculation.

well. This is because both conductor sag and line loading are used in the application to estimate the conductor temperature. The temperature estimated by the state change equation (using conductor sag data as input) and the temperature obtained

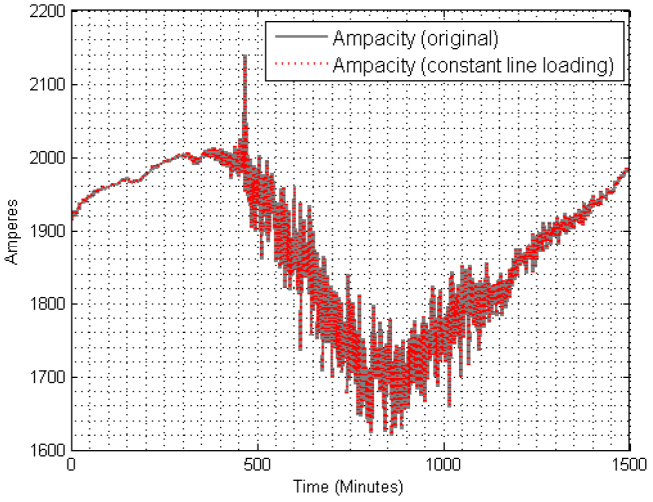

Fig. 12. Impact of line loading in the ampacity calculation.

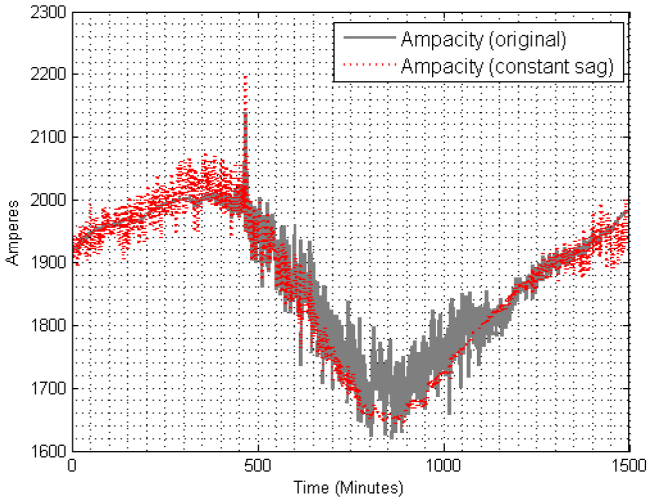

Fig. 13. Impact of sag in the ampacity calculation.

from the IEEE 738 standard (using the line loading and ambient conditions as input) are merged together by the Kalman filter to produce a more reliable estimate. This feature of the algorithm helps the application to tolerate bad data in line loading and conductor sag measurements.

4.3. Comparison with commercial solutions

The output of developed application is next evaluated using measurements from a DLR system on an actual line located close to Liden, Sweden [35]. The real-time ampacity, obtained from the proposed application, has been compared with the ampacities recorded by two commercial temperature-dependent algorithms that were installed on the line as part of the DLR system, as shown in Fig. 14.

Proprietary method 1 (PM1) is a self-constrained method in which a device is mounted directly on the conductor to measure load and conductor temperature. The effective wind acting on the conductor at each site is determined in real-time by a dynamic heat balance formula. The computed wind effect together with the measured load and conductor temperature are used to compute line ratings every minute. The exact algorithm behind this method is undisclosed by the company that produces this system.

Proprietary method 2 (PM2) is based on the IEEE 738 algorithm. The standard is described in detail in [29]. The method considers

the heat balance coefficients (i.e. q_s, q_r, q_c in (1)) using the ambient data from a nearby weather station. In addition, it uses the conductor temperature measured by a sensor mounted on the conductor. Using the measured conductor temperature and the computed heat balance coefficients, the method calculates the ampacity in real-time. Note that, in PM2, the conductor temperature is directly measured and fed to the IEEE 738 algorithm, whereas, in the proposed application, the conductor temperature is estimated from the conductor sag measurements through the state change equation and the Kalman filter. As explained in Sections 1.2 and 4.2, this results in having a less costly but more reliable DLR system.

As shown in Fig. 14, the ampacity calculation from the developed application produces very stable outputs with a much lower variance than the proprietary methods. Thus, it is possible to conclude that the proposed method and software may provide the operator a better estimate of actual line capacity, than these two currently available solutions.

Figs. 15 and 16 show the Probability Density Function (PDF) of the relative difference between the ampacities computed by the developed application and the proprietary methods. The figures are obtained from the data shown in Fig. 14. As Fig. 15 shows, the output of the developed application shows a noticeable relative difference with respect to that of PM1. This is mainly due to the inconsistent output of PM1 during the period of 0–500 min. As shown in Fig. 14, it seems that the method has lost one of its crucial inputs, e.g. the conductor temperature, during this period and therefore it has taken some time before the method can get back to normal operation after the minute of 1100.

In contrast to PM1, PM2 is tracked closely by the developed application, as shown in Fig. 16. As indicated by the figure, the PDF of the relative difference between the outputs of the developed application and PM2 fits a normal distribution with the mean value of 0.027 and standard deviation of 0.1143. The difference between the outputs of the developed application and PM2 is mainly due to two reasons. First, the conductor temperature is obtained differently in these two methods, as mentioned before in this section. Second, the output of PM2 is obtained using the instantaneous wind values (used for the calculation of heat balance coefficients), whereas the minute-mean wind values are used by the developed application (because the ambient data for this case has been revealed to the authors with the resolution of 1 sample per minute).

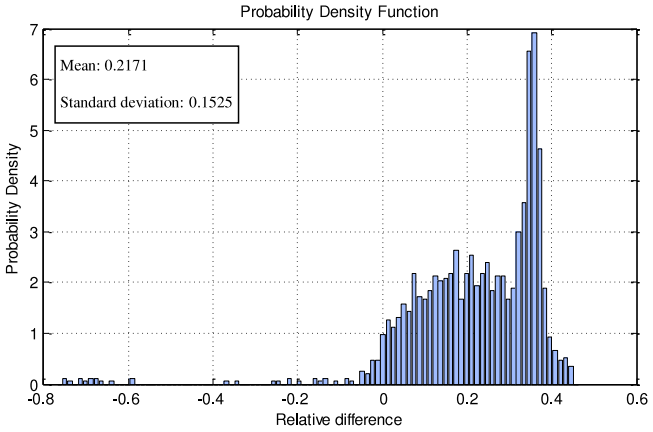

Fig. 15. Probability density function of the relative difference between the outputs of the developed application and the proprietary method 1.

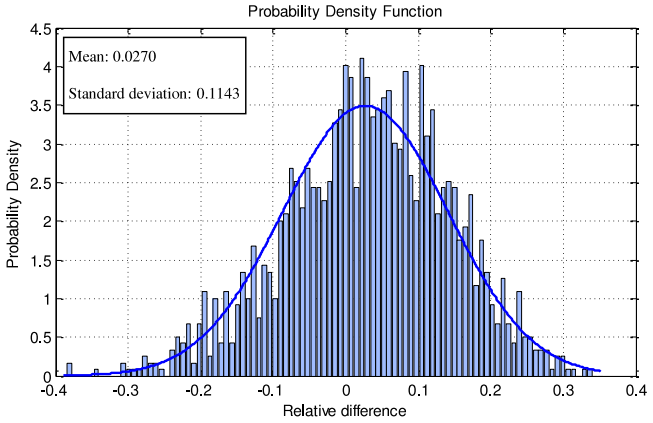

Fig. 16. Probability density function of the relative difference between the outputs of the developed application and the proprietary method 2.

5. Conclusion

This paper presented a dynamic line rating algorithm and software application for active distribution networks. The proposed DLR algorithm acquires data in real-time from weather station (for

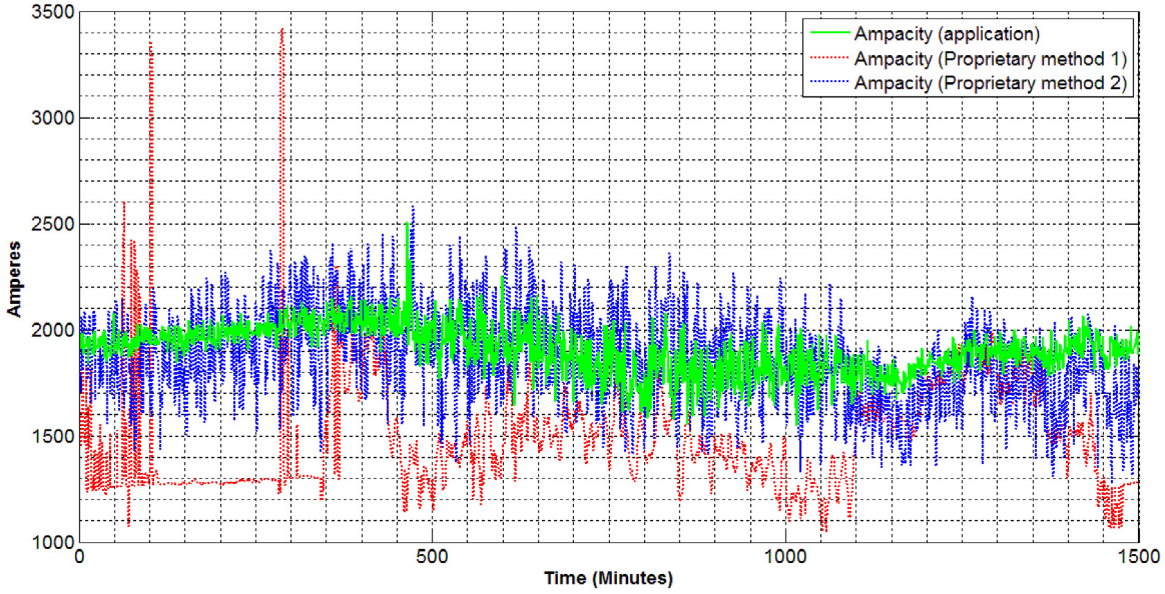

Fig. 14. Comparison of the developed application with two commercial solutions installed on an actual line.

ambient data), PMU (for line loading), and GPS positioning sensor (for conductor sag). The algorithm utilizes a Kalman filter to reliably estimate the conductor temperature based upon which the ampacity is computed for each phase of the line separately, thus being applicable to MV and LV networks where unbalances are present. Comparisons with outputs from two other methods available from field installation in Sweden showed that the proposed application produces very stable outputs with a much lower variance than the proprietary methods. The analyses carried out on the developed application showed its robustness and sensitivity to different input variables under fixed and varying weather conditions.

As future work, the developed application will be further analyzed through block-by-block sensitivity analysis and detailed comparison with available commercial solutions.

Acknowledgment

This work was supported in part by the FP7 IDE4L project funded by the European Commission and the STandUp for Energy Collaboration Initiative.

References

[1] Ec.europa.eu, Statistics Explained, 2015. [Online]. Available: http://ec.europa.eu/eurostat/statistics-explained.
[2] Energy Statistics, 2015. [Online]. Available: http://mospi.nic.in/Mospi_New/upload/Energy_stats_2015_26mar15.pdf.
[3] L.F. Ochoa, C.J. Dent, G.P. Harrison, Distribution network capacity assessment: Variable DG and active networks, IEEE Trans. Power Syst. 25 (1) (2010) 87–95.
[4] C. Mensah-Bonsu, U. Krekeler, G. Heydt, Y. Hoverson, J. Schilleci, B. Agrawal, Application of the Global Positioning System to the measurement of overhead power transmission conductor sag, IEEE Trans. Power Deliv. 17 (1) (2002) 273–278.
[5] M. Andersson Ljus, Dynamic line rating – Thermal line model and control. Lund, 2013.
[6] Dynamic line rating systems for transmission lines. US Department of energy. April 2014. [Online]. Available: https://www.smartgrid.gov/files/SGDP_Transmission_DLR_Topical_Report_04-25-14_FINAL.pdf.
[7] S. Foss, R. Maraio, Evaluation of an overhead line forecast rating algorithm, IEEE Trans. Power Deliv. 7 (3) (1991) 1618–1627.
[8] S. Talpur, C.J. Wallnerstrom, P. Hilber, S.N. Saqib, Implementation of Dynamic Line Rating technique in a 130 kV regional network, in: Multi-Topic Conference, INMIC, 2014 IEEE 17th International, Dec. 2014.
[9] M. Nick, O. Alizadeh-Mousavi, R. Cherkaoui, M. Paolone, Security constrained unit commitment with dynamic thermal line rating, IEEE Trans. Power Syst. 31 (3) (2016) 2014–2025.
[10] S. Abdelkader, S. Abbott, J. Fu, B. Fox, D. Flynn, L. McClean, L. Bryans, Dynamic monitoring of overhead line ratings in wind intensive areas, in: Proc. Eur. Wind Energy Conf. Exhibition, Marseille, France, 2009.
[11] S. Uski, Dynamic line rating forecastability for conservative day-ahead line rating values, in: Industrial Electronics Society, IECON 2015–41st Annual Conference of the IEEE, Yokohama, Japan, 2015, pp. 003738–003742.
[12] I. Bilibin, F. Capitanescu, J. Sachau, Overloads management in active radial distribution systems: An optimization approach including network switching, in: PowerTech, POWERTECH, 2013 IEEE Grenoble, Grenoble, 2013, pp. 1–5.
[13] Dale A. Douglass, F. Ridley Thrash, Electric Power Generation, Transmission, and Distribution, third ed., 2012, pp. 1–42.
[14] R. Henke, S. Sciacca, Dynamic thermal rating of critical lines-a study of real-time interface requirements, IEEE Comput. Appl. Power 2 (3) (1989) 46–51.
[15] A. Bondarenko, Yu. Vasiljev, B. Mekhanoshin, A. Oreshkin, V. Shkaptsov, OHL condition monitoring and engineering solutions to cinch maximum admissible transmitting capacity, in: International Conference on Condition Monitoring and Diagnosis, 2008. CMD 2008, vol., no., 21–24 April 2008, pp. 696–700.
[16] A.K. Deb, Power Line Ampacity System, CRC Press, Boca Raton, 2000.
[17] S. Jupe, M. Bartlett, K. Jackson, Dynamic thermal ratings: The state of art, in: CIRED 21st International Conference on Electricity Distribution, Frankfurt, 6–9 June 2011.
[18] Elena Golinelli, Sergio Musazzi, Umberto Perini, Giovanni Pirovano, Laser based scanning system for high voltage power lines conductors monitoring, in: 20th International Conference and Exhibition on Electricity Distribution - Part 1, 2009. CIRED 2009, vol., no., 8–11 June 2009, pp.1–3.
[19] Ren Lijia, Li Hong, Liu Yan, On-line monitoring and prediction for transmission line sag, in: 2012 International Conference on Condition Monitoring and Diagnosis, CMD, vol., no., 23–27 Sept. 2012, pp. 813–817.
[20] I. Oleinikova, A. Mutule, M. Putnins, PMU measurements application for transmission line temperature and sag estimation algorithm development, in: 55th International Scientific Conference on Power and Electrical Engineering of Riga Technical University, RTUCON, 2014, vol., no., 14–14 Oct. 2014, pp. 181–185.
[21] Mai Rui Kun, Fu Ling, Xu HaiBo, Dynamic Line Rating estimator with synchronized phasor measurement, in: International Conference on Advanced Power System Automation and Protection, APAP, 2011, vol. 2, no., 16–20 Oct. 2011, pp.940–945.
[22] Ruifeng Yan, T.K. Saha, Investigation of voltage imbalance due to distribution network unbalanced line configurations and load levels, IEEE Trans. Power Syst. 28 (2) (2013) 1829–1838.
[23] N.D. Sadanandan, A.H. Eltom, Power donut system laboratory test and data analysis, in: Southeastcon Proceedings IEEE, vol. 2, 1990, pp. 1–4.
[24] J.K. Raniga, R.K. Rayudu, Dynamic rating of transmission lines-a New Zealand experience, in: Power Engineering Society Winter Meeting, 2000. 60 IEEE, vol. 4, no., 2000, pp. 2403–2409.
[25] S. Kamboj, R. Dahiya, Evaluation of DTLR of power distribution line from sag measured using GPS, in: 2011 International Conference on Energy, Automation, and Signal, ICEAS, vol., no., 28–30 Dec. 2011, pp. 1–6.
[26] Dynamic Line Ratings - Nexans, Nexans.us, 2016. [Online]. Available: http://www.nexans.us/eservice/US-en_US/navigate_206113/Dynamic_Line_Ratings.html [Accessed: 30.05.16].
[27] S. User, Avistar Inc. - Span Sentry - Dynamic Line Rating System - Overview, Avistarinc.com, 2016. [Online]. Available: http://www.avistarinc.com/products/span-sentry [Accessed: 30.05.16].
[28] Ampacimon, Ampacimon, 2016. [Online]. Available: http://www.ampacimon.com/ [Accessed: 30.05.16].
[29] IEEE Standard for Calculating the Current-Temperature of Bare Overhead Conductors, IEEE Standard 738–2006 (Revision of IEEE Standard 738–1993), Jan. 2007.
[30] R.E. Pinto, State change equation: Calculation formula, in: 2012 Workshop on Engineering Applications, WEA, vol., no., 2–4, May 2012, pp. 1–5.
[31] P. Maybeck, Stochastic Models, Estimation, and Control, Academic Press, New York, N.Y., 1982.
[32] FP7 IDE4L official website: http://www.ide4l.eu.
[33] H. Hooshyar, F. Mahmood, L. Vanfretti, M. Baudette, Specification, implementation, and hardware-in-the-loop real-time simulation of an active distribution grid, Elsevier J. Sustainable Energy Grids Netw. (SEGAN) 3 (2015) 36–51.
[34] L. Vanfretti, V.H. Aarstrand, M.S. Almas, V.S. Peric, J.O. Gjerde, A software development toolkit for real-time synchrophasor applications, in: Proc. IEEE PowerTech, 2013.
[35] Coordinates of the location: 62° 41′59.6″N16° 48′00.6″E.